Detection of second-order quadrupolar spin-lattice coupling mechanisms in metallic antimony using multifrequency pulsed nuclear quadrupole resonance

J. M. Keartland, G. C. K. Folscher, and M. J. R. Hoch
Condensed Matter Physics Research Unit and Department of Physics, University of the Witwatersrand, Johannesburg, P.O. Wits 2050, South Africa
(Received 3 July 1990; revised manuscript received 1 November 1990)

Semimetals have electronic structures which suggest the possibility of important noncontact terms as well as contact terms in the perturbing Hamiltonian involved in nuclear-spin–lattice relaxation. There is also the possibility of a phonon mechanism becoming important at high temperatures. Experiments using single-frequency and multifrequency pulsed nuclear quadrupole resonance have been carried out on antimony (^{121}Sb) and have permitted electric quadrupolar interaction terms ($\Delta m = \pm 1$ and ± 2) to be separated from the magnetic ($\Delta m = \pm 1$) terms. For temperatures much below the Debye temperature Θ_D, the results suggest that the quadrupolar interaction involving p electrons contributes 5–10 % to the ^{121}Sb relaxation. At temperatures above Θ_D, the importance of the quadrupolar coupling increases dramatically and the ratio of the transition probabilities for $\Delta m = \pm 1$ and $\Delta m = \pm 2$ transitions changes, signaling the emergence of a relaxation mechanism which is probably a two-phonon mechanism.

I. INTRODUCTION

The electronic structures of the group-V semimetals have attracted much attention over the years because of the interesting features which they possess. Both electrons and holes contribute to their electrical properties with carrier densities substantially lower than those in typical metals. The properties of graphite, its compounds, and the group-V semimetals form the subject of a recent two-volume review by Brandt *et al.*[1]

Because of their noncubic crystal structure, and the fact that the nuclei possess quadrupole moments, it is possible to carry out nuclear quadrupole resonance (NQR) experiments in these materials. This paper describes both single-frequency and multifrequency NQR experiments on ^{121}Sb ($I = \frac{5}{2}$) which have obtained information on the various spin-lattice relaxation processes which occur in high-purity antimony. It has previously been suggested by Hewitt and McLaughlin[2] (HM) that both the contact hyperfine interaction and the quadrupole interaction between nuclei and carriers play a role in spin-lattice relaxation processes at low temperatures. These workers used single-frequency methods which were sufficiently accurate at low temperatures ($T = 4.2$ K). The present work has sought to confirm and extend the previous results using a different approach.

Theoretical and experimental studies of the effects of hydrostatic pressure on the electronic structures of the semimetals, particularly antimony, have recently been carried out by a number of workers.[3–5] NQR offers the possibility of probing changes in the electronic structure over a considerable range of pressure. Part of the motivation for the present investigation is to provide a basis for future high-pressure NQR work of this kind on antimony.

The relaxation of ^{121}Sb is governed by an expression involving the sum of two exponentials. Our calculations have shown that a multifrequency pulsed experiment may be utilized to eliminate one of these exponentials. It is further shown that, by fitting a combination of single-frequency and multifrequency experimental data, sufficient information is obtained to permit extraction of all the relevant transition probabilities with adequate precision. Fits to single-frequency data give, in general, a somewhat lower precision. The multifrequency approach has its origins in the early experiments on ^{23}Na in $NaNO_3$ carried out by Pound.[6]

For technical reasons it has been necessary to use a powder sample. Furthermore we have adopted a crossed-coil geometry in order to excite the multifrequency transitions. In establishing the initial conditions appropriate to our analysis it has been necessary to carry out a density-matrix calculation.

Very few examples of quadrupolar relaxation due to carriers in metals have been detected. Narath and Alderman[7] have suggested that this mechanism plays a role in molybdenum where the d-band conduction electrons are probably involved. In antimony the p electrons can provide the coupling. Mitchell's calculations[8] for quadrupolar relaxation in metals have been extended to allow for the nonspherical Fermi surface of antimony.

At temperatures above the Debye temperature ($\Theta_D = 210$ K) it appears likely from the work of Fölscher *et al.*[9] that a phonon-mediated quadrupolar relaxation mechanism becomes increasing important. Further information on this process has been provided by the present work.

II. THEORETICAL CONSIDERATIONS

A. Derivation of the rate equations

Semimetallic antimony crystallizes in the A_7 or arsenic crystal structure, with two atoms per unit cell and an axis

of symmetry along the ⟨111⟩ direction.[10] Two isotopes are present: ^{121}Sb (57% natural abundance; $I=\frac{5}{2}$) and ^{123}Sb (43% natural abundance; $I=\frac{7}{2}$). The interaction between the quadrupole moment of the nucleus and the resulting axially symmetric electric field gradient may be described by the quadrupolar Hamiltonian[11]

$$\mathcal{H}_Q=\frac{1}{4\pi\epsilon_0}\frac{e^2qQ}{4I(2I-1)}(3I_Z^2-I^2)\ . \tag{1}$$

For the ^{121}Sb system this gives rise to two resonance frequencies, denoted $2\omega(\pm\frac{5}{2}\leftrightarrow\pm\frac{3}{2})$ and $\omega(\pm\frac{3}{2}\leftrightarrow\pm\frac{1}{2})$.

The equilibrium population of the nuclear spin states is given by Boltzmann statistics. If this equilibrium population is disturbed, as will be described in the next section, then the nuclear spin system returns to equilibrium via interactions with the lattice. In general we consider a transition from a spin state m to a spin state m', and a transition from a lattice state $\mathbf{k}$ to a lattice state $\mathbf{k}'$. The probability of such a transition is proportional to

$$\sum_{\substack{\mathbf{k}\text{ occupied},\\ \mathbf{k}'\text{ unoccupied}}} |\langle \mathbf{k}'m'|V|\mathbf{k}m\rangle|^2\ ,$$

where the operator V couples the spin and lattice states. V may be written in terms of the nuclear spin operator I as follows:

$$\begin{aligned}
&\Delta m=\pm1 \text{ magnetic } \sqrt{W_m}I_\pm\\
&\qquad\text{quadrupolar } \sqrt{W_{Q1}}(I_\pm I_z+I_zI_\pm)\ ,\\
&\Delta m=\pm2 \text{ quadrupolar } \sqrt{W_{Q2}}I_\pm^2\ ,
\end{aligned}$$

where W_m, W_{Q1}, W_{Q2} are transition rates or the spin-lattice coupling constants. Detailed discussions of these couplings are given in Mitchell[8] (for nucleus-carrier interactions) and van Kranendonk[12] (for nucleus-phonon interactions).

Both $\Delta m=\pm1$ and $\Delta m=\pm2$ transitions may be involved in spin-lattice relaxation for the ^{121}Sb isotope. Rate equations describing spin-lattice relaxation can be written by defining P_m as the deviation of the population of the mth level from an equilibrium (Boltzmann) distribution, and the population difference u_m as

$$u_m=(P_m-P_{m-1})+(P_{-m}-P_{-m+1})\ . \tag{2}$$

McLaughlin *et al.*[13] have shown that a quadrupolar spin system evolves with time according to the matrix differential equation

$$d_tu=Au\ , \tag{3}$$

subject to the appropriate initial conditions.

For an $I=\frac{5}{2}$ system the relaxation matrix A may be written

$$A=\begin{bmatrix}\alpha & \beta\\ \gamma & \delta\end{bmatrix}\ , \tag{4}$$

where

$$\begin{aligned}
\alpha&=-10W_m-160W_{Q1}-40W_{Q2}\ ,\\
\beta&=8W_m+32W_{Q1}+32W_{Q2}\ ,\\
\gamma&=5W_m+80W_{Q1}-40W_{Q2}\ ,\\
\delta&=-16W_m-64W_{Q1}-112W_{Q2}\ .
\end{aligned}$$

The transition rates W_m, W_{Q1}, and W_{Q2} are determined by the spin-lattice coupling. The solution of the matrix differential equation involves the eigenvalues of the relaxation matrix. For the above matrix these may be written as

$$\lambda_{1/2}=\frac{-(\alpha+\delta)\pm\sqrt{\alpha^2+\delta^2+4\gamma\beta}}{2}\ .$$

To solve the matrix differential equation (3), the initial conditions must be determined. We have chosen to use two different sets of initial conditions in order to extract the spin-lattice transition rates by simultaneously fitting two relaxation curves. In general we irradiate at frequencies corresponding to both transitions for ^{121}Sb using a crossed-coiled system. In establishing the initial conditions for this geometry, a density matrix calculation was carried out. Details will be given elsewhere and only the principal results are quoted here.

B. Crossed-coil NQR in a powder sample

The effect on the spin system of a two-pulse sequence at the frequencies $2\omega_0$ and ω_0 has been calculated using the approach of Das and Saha.[14] For convenience the following quantities are defined:

$$\begin{aligned}
x_i&=[(I+m_i)(I-m_i+1)]^{1/2}\ ,\\
\omega_i&=\frac{\langle m_iI|\mathcal{H}_Q|m_iI\rangle}{\hbar}\ ,\\
\tau_i&=\text{width of the } i\text{th pulse}\ ,
\end{aligned}$$

where $m_1=\frac{5}{2}$; $m_2=\frac{3}{2}$.

The effects of spin-lattice relaxation and spin-spin relaxation on the elements of the density matrix are introduced in the usual way[15] by means of the following assumptions: (a) the diagonal elements of $\rho(t)$ relax to equilibrium with the effective spin-lattice relaxation time T_1; (b) the off-diagonal elements decay to zero with time constant T_2 where $T_1\gg T_2$.

Calculation of the density matrix, after a two-pulse sequence where the spacing between the pulses, t, is such that $T_2<t\ll T_1$, and where a further time t is allowed to elapse after the second pulse, is accomplished using the above assumptions.

For a powder sample the diagonal elements of the density matrix must be averaged over all possible crystallite orientations. This involves averaging terms of the form $\cos(\sin\theta)$ and $\cos(\sin^2\phi+\cos^2\phi\cos^2\theta)^{1/2}$ over a sphere. Bessel function expansions[16] are utilized. The two 6×6 matrices obtained are symmetrical, and may be rewritten in terms of the equilibrium population of the $\pm\frac{1}{2}$ level, p_0, giving two 3×3 matrices:

$$\rho_1(t)=p_0\begin{bmatrix}1-\beta\Delta[2+\mathcal{J}(x_1\omega_1\tau_1)] & 0 & 0\\ 0 & 1-\beta\Delta[2-\mathcal{J}(x_1\omega_1\tau_1)] & 0\\ 0 & 0 & 1\end{bmatrix},$$

$$\rho_2(2t)=p_0\begin{bmatrix}1-\beta\Delta[2+\mathcal{J}(x_1\omega_1\tau_1)] & 0 & 0\\ 0 & 1-\frac{1}{2}\beta\Delta[2-\mathcal{J}(x_1\omega_1\tau_1)][1+\mathcal{J}(x_2\omega_2\tau_2)] & 0\\ 0 & 0 & 1-\frac{1}{2}\beta\Delta[2-\mathcal{J}(x_1\omega_1\tau_1)][1-\mathcal{J}(x_2\omega_2\tau_2)]\end{bmatrix},$$

where

$$\mathcal{J}(x)=\sum_{n=0}^{\infty}\frac{J_{2n}(x)}{1-4n^2},$$

and the J's are Bessel functions.

The size of a quadrupolar spin echo produced by a two-pulse sequence with spacing $t'\ll T_2$ is proportional to the difference in population between the two irradiated levels. This idea is the basis for all relaxation measurements. The application of such a pulse sequence at frequency 2ω at times t and $2t$ will produce echoes given by

$$M(t)=V_0\mathcal{J}(x_1\omega_1\tau_1),$$

$$M(2t)=\tfrac{1}{4}V_0\{2[1-\mathcal{J}(x_2\omega_2\tau_2)]+\mathcal{J}(x_1\omega_1\tau_1)[3+\mathcal{J}(x_2\omega_2\tau_2)]\},\quad(5)$$

where V_0 is the size of the echo when the two "saturation" pulses are removed. These expressions will be used in setting the appropriate pulse widths for the initial conditions, which are calculated below.

C. Determination of initial conditions

The initial conditions for the two kinds of experiments carried out are determined with reference to the results of the density matrix calculation. A pulse is applied at frequency 2ω so that a number of spins, $p_0\nu$, in the $\pm\frac{3}{2}$ level are excited into the $\pm\frac{5}{2}$ level. At a time t ($T_2<t\ll T_1$) later, a pulse at frequency ω is applied so that a number of spins, $p_0\mu$, in the $\pm\frac{1}{2}$ level are excited into the $\pm\frac{3}{2}$ level. The initial condition becomes

$$u(0)=\begin{bmatrix}2\nu-\mu\\ 2\mu-\nu\end{bmatrix}.\quad(6)$$

In terms of the results of the density matrix calculation

$$\nu=\beta\Delta[1-\mathcal{J}(x_1\omega_1\tau_1)]\quad(7a)$$

and

$$\mu=\tfrac{1}{2}\beta\Delta[2-\mathcal{J}(x_1\omega_1\tau_1)][1-\mathcal{J}(x_2\omega_2\tau_2)].\quad(7b)$$

The general solution for (4) is written as

$$u(t)=U\,\mathrm{diag}[\exp(\lambda_1 t),\exp(\lambda_2 t)]U^{-1}u(0),$$

where

λ_1,λ_2 are eigenvalues of the relaxation matrix A,

U is the matrix of eigenvectors of A.

This may be rewritten as

$$u(t)=\frac{1}{\lambda_1-\lambda_2}\begin{bmatrix}C & D\\ E & F\end{bmatrix}\begin{bmatrix}\exp(\lambda_1 t)\\ \exp(\lambda_2 t)\end{bmatrix},$$

where

$$C=(\alpha-\lambda_2)(2\nu-\mu)+\beta(2\mu-\nu),$$

$$D=(\lambda_1-\alpha)(2\nu-\mu)-\beta(2\mu-\nu),$$

$$E=(\delta-\lambda_2)(2\mu-\nu)+\gamma(2\nu-\mu),$$

$$F=(\lambda_1-\delta)(2\mu-\nu)-\gamma(2\nu-\mu).$$

In the experiment described in the next section the $\pm\frac{5}{2}\leftrightarrow\pm\frac{3}{2}$ transition is monitored. Recovery to equilibrium is described by

$$u_{5/2}(t)=\frac{1}{\lambda_1-\lambda_2}\left[Ce^{\lambda_1 t}+De^{\lambda_2 t}\right].\quad(8)$$

For a negligible quadrupolar contribution to relaxation ($W_{Q1}\simeq W_{Q2}\simeq 0$) this reduces to

$$u_{5/2}(t)=\tfrac{1}{7}[3(2\nu+\mu)\exp(-6W_m t)+2(4\nu-5\mu)\exp(-20W_m t)],\quad(9)$$

where, from Eq. (7b), $\mu=0$ in the single-frequency experiment.

The coefficient D of the second exponential in Eq. (9) may be made to vanish in the double frequency experiment by arranging that $4\nu=5\mu$. Results of the density matrix calculation given in the previous section may be used to obtain the appropriate condition in terms of rf pulse lengths. If the first pulse is set such that $\mathcal{J}(x_1\omega_1\tau_1)=0$, then, using Eqs. (7), we obtain

$$\frac{\mu}{\nu}=\frac{4}{5}=1-\mathcal{J}(x_2\omega_2\tau_2)$$

or

$$\mathcal{J}(x_2\omega_2\tau_2)=\tfrac{1}{5}.\quad(10)$$

This condition may be established experimentally using procedures described in the following section.

It is appropriate to consider the effects of quadrupolar contributions to relaxation on the condition $D=0$. The general form of the relation between μ and ν required to satisfy this condition for arbitrary values of W_m, W_{Q1}, and W_{Q2} is

$$\frac{\mu}{\nu}=\frac{2\{1+54\kappa-96\chi+[9(1-16\kappa+12\chi)^2+40(1+4\kappa+4\chi)(1+16\kappa-8\chi)]^{1/2}\}}{13+112\kappa-48\chi+[9(1-16\kappa+12\chi)^2+40(1+4\kappa+4\chi)(1+16\kappa-8\chi)]^{1/2}},$$

where

$$\kappa=\frac{W_{Q1}}{W_m},\quad \chi=\frac{W_{Q2}}{W_m}.$$

In the low-temperature regime ($T \ll \Theta_D$), where the results of HM suggest that $\kappa \leq 0.01$ and $\chi \leq 0.01$, the condition given by Eqs. (10) can be used directly. In the curve fitting procedures μ and ν may be allowed to vary over a limited range to allow for experimental uncertainties in setting the pulse and also possible small quadrupolar relaxation effects.

At higher temperatures ($T \geq \Theta_D$), where it appears that κ and χ are not small, the complete expression Eq. (8) should be used in setting the initial conditions. In principle the three relaxation contributions could be determined using an iterative procedure involving curve fitting and adjustments to the initial conditions. We have not done this but have assumed W_m is known from the Korringa relation and values of W_m obtained at lower temperatures. The condition $D=0$ is then approximately satisfied and W_{Q1} and W_{Q2} may be determined by curve fitting to both single and double frequency relaxation data and by allowing μ and ν some freedom to vary. Our results indicate that the method is sensitive to relatively small increases in W_{Q1} and W_{Q2}. This is due to the effects of the large coefficients of terms involving these quantities in the relaxation expression. By demanding consistency in the fitting parameters for the single and double frequency experiments it is possible to determine the presence of quadrupolar terms of the order of a few percent. An upper limit may be placed on quadrupolar contributions less than this.

III. EXPERIMENTAL APPARATUS AND TECHNIQUE

Measurements were made using a variable frequency, coherent, pulsed NQR spectrometer with two transmitter channels operating at frequencies ω and 2ω. The frequency source was a crystal-locked HP 3335A synthesizer operating at frequency ω. A frequency doubler was used to obtain frequency 2ω. By means of a crossed-coil arrangement it was possible to excite both $\pm\frac{1}{2}\leftrightarrow\pm\frac{3}{2}$ and $\pm\frac{3}{2}\leftrightarrow\pm\frac{5}{2}$ transitions. The coil geometry for the cylindrical Helmholtz coil, used for the lower frequency transition, was chosen to optimize the homogeneity of the rf field.[17]

The antimony sample used was 99.9999% shot obtained from Koch-Light U.K. It was crushed to 25μ mesh and annealed for 4 h at 525 °C. Following annealing, the material was gently separated and sealed in a Pyrex ampoule under vacuum. It was found to be unnecessary to separate the antimony grains using fine quartz powder, although this was utilized in preliminary experiments.

Temperature control was achieved by immersing the sample in constant temperature baths—liquid nitrogen, melting ice, and paraffin oil at ambient temperature. Heating effects due to the rf pulses were found to be negligibly small even at 77 K.

Signal averaging was carried out using a Tektronix 468 oscilloscope which was interfaced to an HP 85 desk-top computer. A nine-point smoothing routine and baseline corrections were applied to the echo before the echo amplitude was measured. A signal-to-noise ratio of better than 50:1 was achieved without difficulty at 77 K, and this degraded to 15:1 at the higher temperatures. Reproducibility of signals was within a few percent.

The setting of appropriate saturating pulses for the experiment was accomplished empirically. The full saturation pulse at frequency 2ω was determined by applying a Θ pulse (at 2ω) followed at a time $t \ll T_1$ later by a two-pulse quadrupolar echo generating sequence (at 2ω). The echo amplitude was measured as a function of the width of the pulse (τ_1) and the data fitted to a curve of the form $V_0 J(k\tau_1)$ [see Fig. 1(a)]. The pulse was set at full satura-

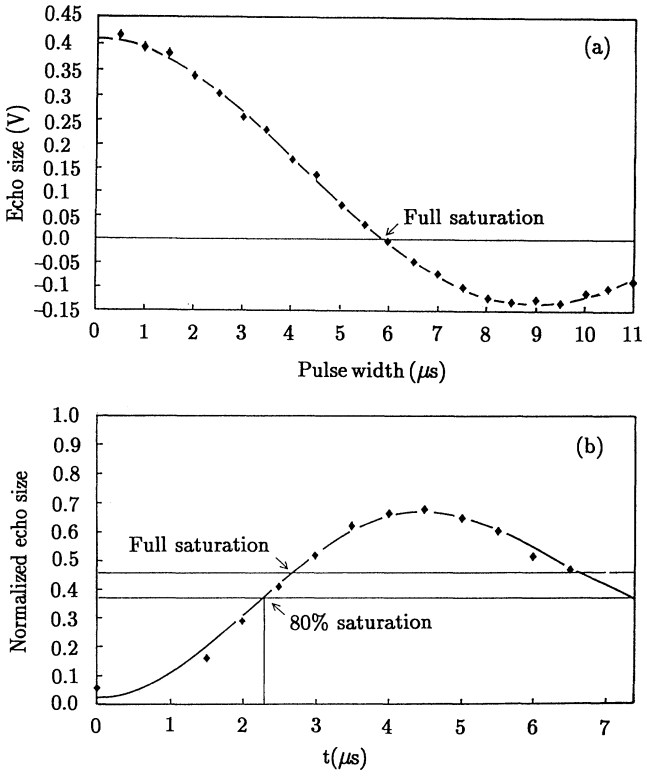

FIG. 1. (a) Pulse setting curve for the $\pm\frac{5}{2}\leftrightarrow\pm\frac{3}{2}$ transition. Data is fitted with a curve of the form $V_0 J_0(k\tau_1)$. (b) Pulse setting curve for the $\pm\frac{3}{2}\leftrightarrow\pm\frac{1}{2}$ transition. Data is fitted with a curve of the form $V_0[1-J_0(k\tau_2)]$. The condition for 80% saturation is determined graphically as indicated.

tion, as indicated in Fig. 1(a), for the rest of the experiment. The single-frequency relaxation data were then gathered in the usual way. The 80% saturation pulse at frequency ω was then determined. The full saturation pulse was applied at frequency 2ω, followed by a Θ pulse at ω a time t_1 ($\ll T_1$) later followed by an echo generating sequence (at 2ω). The echo amplitude was measured as a function of the width of the Θ pulse (τ_2), and the data fitted to a function of the form $V_0[1-J_0(k\tau_2)]$ [see Fig. 1(b)]. The pulse was set at 80% saturation, as indicated in Fig. 1(b), for the rest of the experiment. The two-frequency relaxation data were then gathered, keeping the time between the first two pulses (t_1) constant.

IV. EXPERIMENTAL RESULTS

Representative relaxation data obtained at 77 K using the single and double frequency methods are shown (plotted points) in Fig. 2. Curves were fitted to the experimental results using two different procedures. Firstly (procedure 1) negligible quadrupolar relaxation was assumed ($W_{Q1}=W_{Q2}=0$) and W_m was determined by fitting Eq. (9) to the data. Secondly (procedure 2) quadrupolar terms were included and Eq. (8) was used to fit the two sets of data simultaneously employing the appropriate expressions for λ_1 and λ_2. We put $\mu/\nu=0.8$ for the double frequency data as this condition can be set quite well when magnetic processes are dominant. The results obtained are shown in Table I.

From Table I it can be seen that methods 1 and 2 give reasonably consistent values for W_m. This implies that the quadrupolar terms play, at most, a small role in relaxation at 77 K. Method 2 allows an estimate to be made of W_{Q1} and W_{Q2}. We obtain $W_{Q1}/W_{Q2}=1.75$ and $W_{Q1}/W_m=\kappa=0.70\%$. These values are consistent with the estimates given by HM. It should be borne in mind that, while W_{Q1} and W_{Q2} are less than 1% of W_m, the coefficients W_{Q1} and W_{Q2} in the expressions for λ_1 and λ_2 are quite large compared to those for W_m and this can give rise to detectable effects in relaxation. While the values for W_{Q1} and W_{Q2} given in Table I should be regarded with some caution, the evidence indicates that a small quadrupolar contribution is present. The fits to the data obtained when W_{Q1} and W_{Q2} were included resulted in a 15% decrease in the least-squares χ^2 value compared to that obtained when they were set equal to zero.

W_m values were also obtained at 77 K for the ^{123}Sb ($\frac{7}{2}-\frac{5}{2}$) transitions by assuming negligible quadrupolar relaxation. The ratio of these two values for W_m differed from the γ^2 ratio by 5±2%. The signal obtained using the ^{123}Sb nucleus was poor in comparison with the signal from the ^{121}Sb nucleus, and this led to the fairly large experimental uncertainty. HM obtained a difference of 10% between the γ^2 ratio and the ratio of the experimentally obtained W_m values. The present results indicate that the quadrupolar contribution may be smaller than that measured by HM.

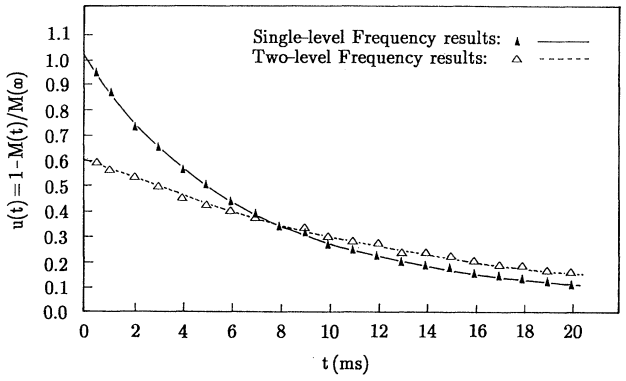

FIG. 2. Relaxation curves for single-level and multilevel experiments at 77 K. Curves shown are the result of simultaneously fitting the data with the theoretically determined multiexponential expressions.

The relaxation data obtained at higher temperatures were fitted using procedures somewhat modified from those used at 77 K. Preliminary fits showed that the quadrupolar contributions were significant. This made it difficult to set μ/ν exactly and it was decided to allow this quantity to have some freedom in the fitting procedure. In order to reduce the number of variables, W_m was fixed using the Korringa relation together with the mean value obtained for this quantity at 77 K. Table II shows the results of the simultaneous fitting procedures carried out on data at 273 and 295 K. Considerably better fits were obtained with the quadrupolar terms included than with them excluded. An improvement of 25% in the χ^2 value was found in both cases.

TABLE I. Transition rates W_m, W_{Q1}, and W_{Q2} determined using least-squares fits to the 77-K data. Details of the two fitting methods are described in the text. In method 1 W_{Q1} and W_{Q2} are put equal to zero.

T (K)		$W_m(s^{-1})$	$W_{Q1}(s^{-1})$	$W_{Q2}(s^{-1})$
77 K	Method 1 (see text)			
	Curve A (Fig. 2)	11.7±0.1		
	Curve B (Fig. 2)	11.6±0.1		
77 K	Method 2 (see text) (simultaneous fit to curves *A* and *B*)	10.4±0.1	0.073±0.004	0.042±0.002

TABLE II. Transition rates determined using least-squares fits to the data obtained at 273 and 295 K. The values for W_m at these temperatures were fixed using the Korringa relation and the 77-K value.

		$W_m(s^{-1})$ (Fixed using Korringa relation)	$W_{Q1}(s^{-1})$	$W_{Q2}(s^{-1})$
273 K	Simultaneous fit	(36.8)	1.6±0.3	2.0±0.3
295 K	Simultaneous fit	(39.8)	1.8±0.3	2.1±0.3

V. DISCUSSION

The results of Fölscher *et al.*[9] and HM have demonstrated that the dominant contribution to spin-lattice relaxation for temperatures below Θ_D is due to the carriers near the Fermi surface (FS). Four types (three, magnetic; one, electric) of nucleus-carrier interaction have been identified in the literature[3,10]

Contact spin	(W_c),	
Noncontact spin	(W_D),	
Noncontact orbital	(W_L),	magnetic;
Quadrupolar	(W_{Q1} and W_{Q2}),	electric.

note: $W_m = W_c + W_D + W_L$.

As mentioned above, HM have made relaxation measurements on the ^{121}Sb and ^{123}Sb isotopes which, together with the gyromagnetic ratios, suggest that a quadrupolar mechanism plays a role in relaxation at 4 K. They found that the W_m ratios for the two isotopes differ from the γ^2 ratio by roughly 10%. We have made similar isotope measurements at 77 K, which indicate that this difference is somewhat lower (approximately 5%). HM analyzed their 4-K data by expanding the exponentials in their relaxation expression and by retaining only linear terms in W_m, W_{Q1}, and W_{Q2}. They then forced the ratios of these quantities for the two isotopes to follow the γ^2 (magnetic) and $\{Q[I(2I-1)]\}^2$ (quadrupolar) ratios. By simultaneously fitting three relaxation curves using the linearized relaxation expression, they were able to determine W_m, W_{Q1}, and W_{Q2} for each isotope. The linearization procedure is clearly only approximate and its validity becomes increasingly questionable as the temperature is raised. We have therefore not pursued this method any further.

In estimating the relative importance of the various relaxation contributions it is necessary to introduce carrier wave functions. The carrier wave function used by Mitchell[3] and of the form suggested by Bardeen[18] is

$$\psi_{\mathbf{k}}(\mathbf{r}) = u_{\mathbf{k}}(r) + i\mathbf{k}\cdot\mathbf{r}v(r) ,$$

where $u_{\mathbf{k}}(r)$ and $v(r)$ are radial s- and p-wave functions. This may be used to calculate each of the above spin-lattice coupling parameters which may be written in terms of sums over occupied momentum states $\mathbf{k}$ and the unoccupied states $\mathbf{k}'$ as follows:

$$W_c = \left[\frac{\mu_0}{4\pi}\frac{8\pi}{3}\mu_B g\mu_N\right]^2 \sum_{\mathbf{k},\mathbf{k}'} |u_{\mathbf{k}}(0)|^2\,|u_{\mathbf{k}'}(0)|^2 ,$$

$$W_D = \left[\frac{\mu_0}{4\pi}\frac{\mu_B g\mu_N}{5}B\right]^2 \sum_{\mathbf{k},\mathbf{k}'} [\tfrac{1}{9}|a_1(\mathbf{k},\mathbf{k}')|^2 + \tfrac{1}{4}|a_2(\mathbf{k},\mathbf{k}')|^2 + 4|a_3(\mathbf{k},\mathbf{k}')|^2] ,$$

$$W_L = \left[\frac{\mu_0}{4\pi}\frac{\mu_B g\mu_N}{6}B\right]^2 \sum_{\mathbf{k},\mathbf{k}'} |a_4(\mathbf{k},\mathbf{k}')|^2 ,$$

$$W_{Q1} = \left[\frac{1}{4\pi\epsilon_0}\frac{e^2Q}{20I(2I-1)}B\right]^2 \sum_{\mathbf{k},\mathbf{k}'} |a_2(\mathbf{k},\mathbf{k}')|^2 ,$$

$$W_{Q2} = \left[\frac{1}{4\pi\epsilon_0}\frac{e^2Q}{20I(2I-1)}B\right]^2 \sum_{\mathbf{k},\mathbf{k}'} |a_3(\mathbf{k},\mathbf{k}')|^2 ,$$

where μ_B is the Bohr magneton, g the nuclear g factor, and μ_N the nuclear magneton. We define $B = \int(|v(r)|^2/r)d\tau$ and $Q = Q_0(1-\gamma_\infty)$, where Q_0 is the nuclear quadrupole moment, γ_∞ the Sternheimer antishielding factor, and e the electronic charge.

The quantities in the summations are defined as

$$|a_1(\mathbf{k},\mathbf{k}')|^2 = (3k_z'k_z - \mathbf{k}'\cdot\mathbf{k})^2 ,$$

$$|a_2(\mathbf{k},\mathbf{k}')|^2 = (k_z'k_x + k_x'k_z)^2 + (k_y'k_z + k_z'k_y)^2 ,$$

$$|a_3(\mathbf{k},\mathbf{k}')|^2 = (k_x'k_x - k_y'k_y)^2 + (k_x'k_y + k_y'k_x)^2 ,$$

$$|a_4(\mathbf{k},\mathbf{k}')|^2 = (k_y'k_z - k_z'k_y)^2 + (k_z'k_x - k_x'k_z)^2 .$$

The FS of antimony consists of three pockets of electrons and six pockets of holes situated around the L and T points of crystal symmetry respectively.[19] These pockets may be approximated by ellipsoids, which are tilted with respect to the trigonal axis of the crystal.

The contributions due to spin-lattice relaxation from the p-wave carriers (W_D, W_L, W_{Q1}, W_{Q2}) have been calculated using FS parameters in the literature.[19] Interellipsoid scattering of either carrier was assumed, but electron-hole interactions were ignored. Details of these calculations will be provided elsewhere.

The ratio between the two quadrupolar relaxation rates is of some interest, since this ratio has been measured by the method described in this work, and by HM using a somewhat different approach. The predicted ratio $W_{Q1}/W_{Q2} \simeq \frac{1}{2}$ differs markedly from the measured values. The reason for this discrepancy is not clear, since the two measured values are reasonably close. A detailed comparison of the experimental results is not possible, as HM do not offer error estimates.

The ratio between the quadrupolar and noncontact magnetic interactions is also of some interest, and provides information on the Sternheimer antishielding factor, γ_∞. Estimates in the literature[20] give

$$1 \leq 1-\gamma_\infty \leq 15 .$$

A lower bound can be placed on $1-\gamma_\infty$ using the results of this work.

Thus,

$$\frac{W_{Q1}+W_{Q2}}{W_L+W_D} \geq 1.1\times 10^{-2}$$

from the experimental results and

$$\frac{W_{Q1}+W_{Q2}}{W_L+W_D} \simeq (1-\gamma_\infty)^2 7\times 10^{-4}$$

from the theoretical calculations leading to

$$1-\gamma_\infty \geq 4.0 .$$

The ratio of the contact and noncontact contributions may be calculated using the available free atom wave functions of Herman and Skillman.[21]

The results obtained at the higher temperatures (273 and 295 K) show a large increase in the quadrupolar spin-lattice coupling. This is consistent with the high-temperature data of Folscher *et al.*[9] and may be ascribed to a two-phonon (Raman) process. The ratio W_{Q1}/W_{Q2} can be estimated as 0.6 (after the low-temperature contributions have been subtracted). The two-phonon quadrupolar contribution is dependent on the phonon density of states and the crystal symmetry. Calculations of Raman spin-lattice coupling constants using a Debye approximation to the phonon density of states have been given by van Kranendonk[12] and Mieher[22] for the NaCl and ZnS lattices, respectively. W_{Q1}/W_{Q2} is estimated as $\simeq 2$ for NaCl, and $\simeq 1$ for ZnS. The present measured value for a rhombohedral structure is lower than either of these figures. The present results strongly suggest that the nature of the relaxation mechanism for $T > \Theta_D$ is quite different from that found at lower temperatures and this supports the proposed phonon mechanism at high temperatures.

VI. CONCLUSION

The use of a multifrequency pulsed NQR for detecting second-order spin-lattice coupling mechanisms, and for determining transition probabilities with adequate precision has been demonstrated. Detailed calculations necessary for establishing the procedures used in experimental measurement and for data analysis have been carried out. These methods should be applicable to a number of systems.

Measurements made on ^{121}Sb in high-purity antimony show that the quadrupolar mechanism, involving interactions with the charge carriers, which was suggested by HM to explain their 4-K results, plays a small but detectable role in relaxation at temperatures below Θ_D. We have been able to determine this contribution at 77 K where the approach of HM becomes marginal. Our results suggest that the quadrupolar mechanism contributes 5–10% to the total relaxation process. The dominant contribution to spin-lattice coupling would seem to be the s-wave contact interaction, but there appears to be a fairly significant p-wave contribution as well. This is the only system, to our knowledge, that exhibits such behavior. The quadrupolar effect could be comparable in the other rhombohedral semimetals, arsenic and bismuth.

At higher temperatures ($T > \Theta_D$) the present results confirm a previous suggestion[9] that another relaxation mechanism becomes important. In this temperature range the $\Delta m = \pm 1$ and $\Delta m = \pm 2$ transition probabilities may be compared. It is not possible to compare the measured ratio with theoretical predictions based on, say, a point charge model as these have not yet been carried out for a rhombohedral lattice. This ratio is, however, consistent with predictions for the fcc and zinc-blende-structure lattices.

[1] N. B. Brandt, S. M. Chudinov, and Ya. G. Ponomarev, *Semimetals—Modern Problems in Condensed Matter Sciences,* edited by V. M. Agranovich and A. A. Maradudin (North-Holland, Amsterdam, 1988), Vols. 20.1 and 20.2.

[2] R. R. Hewitt and D. E. McLaughlin, J. Mag. Res. **30**, 83 (1978).

[3] Yu. A. Pospelov, JETP Lett. **29**, 192 (1979).

[4] Yu. A. Pospelov and G. S. Grachev, J. Phys. F **13**, 179 (1983).

[5] A. A. Abd El Rahman and W. R. Datars, Phys. Rev. B **33**, 7902 (1986).

[6] R. V. Pound, Phys. Rev. **79**, 685 (1950).

[7] A. Narath and D. W. Alderman, Phys. Rev. **143**, 328 (1966).

[8] A. H. Mitchell, J. Chem. Phys. **26**, 1714 (1957).

[9] G. C. K. Folscher, M. J. R. Hoch, and A. Tzalmona (unpublished).

[10] R. W. G. Wyckoff, *Crystal Structures* (Wiley, New York, 1963).

[11] C. P. Slichter, *Principles of Magnetic Resonance* (Harper and

Row, New York, 1963).
[12]J. van Kranendonk, Physica **20**, 781 (1954).
[13]D. E. McLaughlin, J. D. Williamson, and J. Butterworth, Phys. Rev. B **4**, 60 (1971).
[14]T. P. Das and A. K. Saha, Phys. Rev. **98**, 516 (1955).
[15]A. Abragam, *The Principles of Nuclear Magnetism* (Oxford University Press, New York, 1968).
[16]M. R. Spiegel, *Mathematical Handbook* (McGraw-Hill, New York, 1968).
[17]P. Mansfield and P. G. Morris, *NMR Imaging in Biomedicine* (Academic, New York, 1982).
[18]J. Bardeen, J. Chem. Phys. **6**, 367 (1938).
[19]M. S. Dresselhaus, in *Proceedings of Conference on The Physics of Semimetals and Narrow-Gap Semiconductors, Dallas, 1970* (Pergamon, Oxford, 1971).
[20]E. H. Hygh and T. P. Das, Phys. Rev. **143**, 452 (1966).
[21]F. Herman and S. Skillman, *Atomic Structure Calculations* (Prentice-Hall, Englewood Cliffs, New Jersey, 1963).
[22]R. L. Mieher, Phys. Rev. **1255**, 1537 (1962).